

Behavior of bubble induced by fiber-type laser for TUL near soft wall with deformability

¹Yasuhiro Sugimoto*; ²Daichi Nagata; ¹Keiichi Sato;

¹*Kanazawa Institute of Technology, Ishikawa, JAPAN*

²*Graduate School of Kanazawa Institute of Technology, Ishikawa, JAPAN*

Abstract

A fiber-type laser induced bubble makes an important role on laser lithotripsy. This treatment can be affected by the circumference condition such as ureter tissue and a stone. In this study, we observed behavior of the bubble in a narrow space between two walls with different deformability. According to the present experimental results, a bubble symmetrically divides into two parts and collapses in the case of two walls with same hardness. The soft wall is deformed with bubble growth and collapse. In the case of walls with different hardness materials, the bubble which shows characteristic behavior asymmetrically divides, moves and collapses even if the bubble is formed at the center of two walls. The bubble moves toward wall direction during multiple collapses. The larger bubble collapse on the hard wall, that is, the impact is predicted to be larger on the rigid wall. It is found that bubble collapse pattern is greatly affected even by slight wall deformation.

Keywords: Laser-induced bubble; Bubble behavior; Bubble collapse position; Soft wall behavior; Ho:YAG laser.

Introduction

Transurethral ureterolithotripsy (TUL) is effectively carried out by means of pulsed Holmium: YAG laser [1]-[2]. A single bubble is formed at a fiber tip when a laser with high absorption rate irradiates into water through an optical fiber. The bubble shows characteristic behavior when it grows and collapses. Shock waves generated at the bubble collapse act on the stone. The bubble collapse and shock wave behavior play an important role on the lithotripsy.

We have studied the behavior of a bubble induced by the fiber type laser [3]-[4]. The bubble behavior was observed by a high speed video camera simultaneously with impulse force measurement using a hand-made sensor for various laser irradiation conditions. As a result, in the case of a bubble generated near a solid wall, the bubble collapses not at the fiber tip but on the wall and causes the maximum impact on wall surface at a certain distance from the wall to the fiber tip. It is pointed out that there is an optimum laser irradiation condition on the wall impact for TUL.

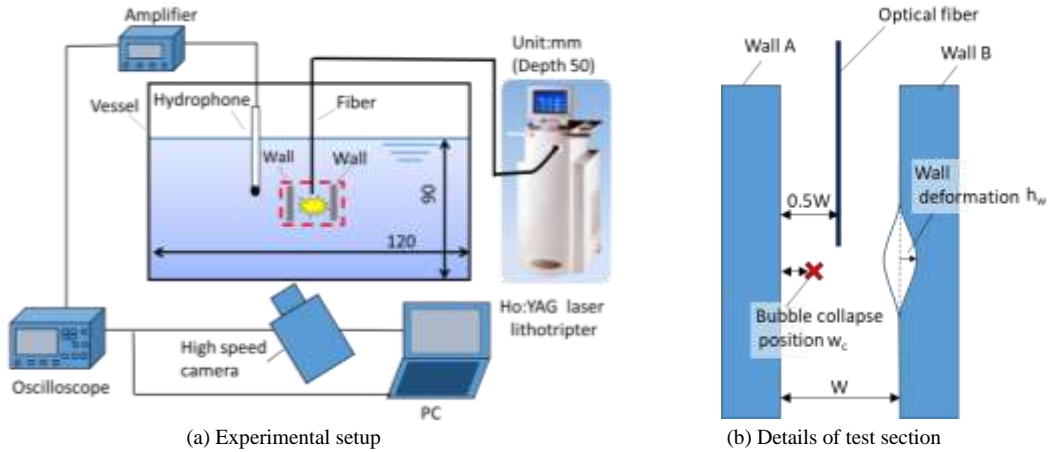
In general, this laser surgery is carried out in a narrow space with a soft material such as kidney and ureter tissue. There are some studies on behavior near an elastic wall [5], near soft and rigid boundaries [6], between two rigid walls [7], and with stone motion [8]. It is important to understand the bubble behavior and their impact mechanism in narrow space that simulates in vivo condition because there is a possibility to be injured by its impact on the tissue.

In the present study, we observe behavior of bubble in a narrow space composed of two plates with deformability.

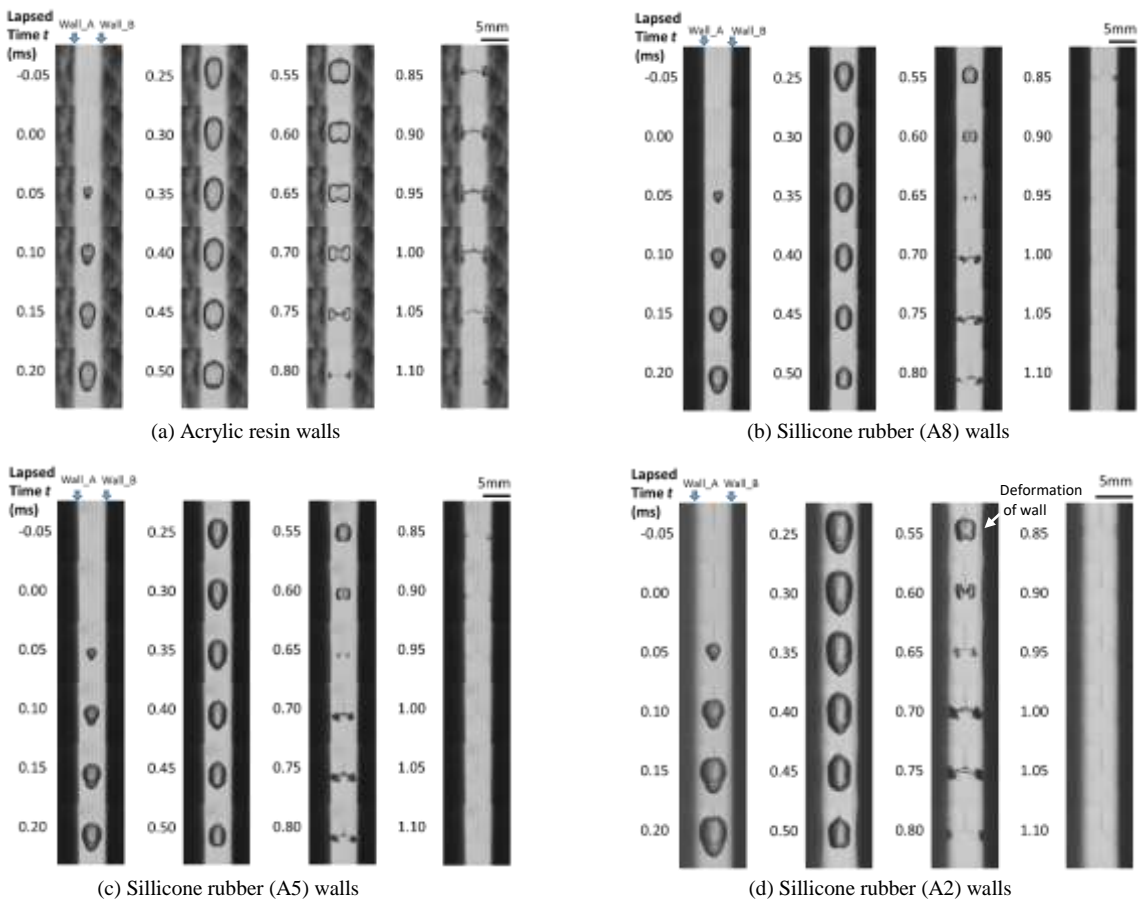
Experimental apparatus and procedure

Experimental setup is shown in Fig. 1. Laser irradiates from a clinical laser lithotripter (Ho:YAG, $\lambda = 2.06 \mu\text{m}$, Pulse duration $\tau = 0.25 \text{ ms}$, Lumenis, VersaPulse Select 30W) through an optical fiber ($d = 0.2 \text{ mm}$, Boston Scientific Japan, Flexiva 200) to a test section between two walls inside a vessel. The two walls which consist of rigid (made of acrylic resin) and/or soft (made of silicone rubber with durometer A hardness of 2, 5 and 8) materials are kept $W = 5 \text{ mm}$ apart. Hardness of silicone rubber is soft in order by A2, A5 and A8 (A2 is almost equivalent to human skin). The optical fiber is installed in the center between two walls. A bubble size is controlled by the laser power. The bubble behavior is observed by a high-speed video camera (Photron, SA5, Spatial resolution: 0.05 mm/pixel) triggered by an output of hydrophone (B&K, 8103). The bubble is illuminated by a light source (NPI, PCS-MH375RC) with a flat light guide (NPI, PLG-B100X) placed behind the test section.

*Corresponding Author, Yasuhiro Sugimoto: y-sugi@neptune.kanazawa-it.ac.jp



(a) Experimental setup
 (b) Details of test section
 Fig.1 Experimental setup and test section



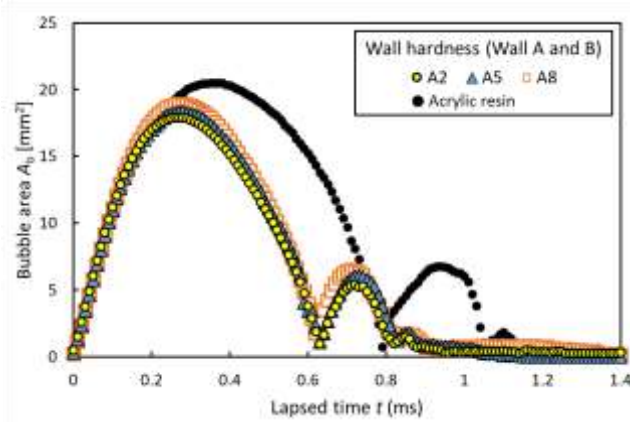
(a) Acrylic resin walls
 (b) Silicone rubber (A8) walls
 (c) Silicone rubber (A5) walls
 (d) Silicone rubber (A2) walls
 $E = 1.0 \text{ J}$, $d = 0.2 \text{ mm}$, $T_w = 297 \text{ K}$, $\beta = 7.8 \text{ mg/L}$, $f_s = 100,000 \text{ fps}$
 Fig.2 Behavior of bubble between two walls with same hardness

Bubble behavior between two walls with the same hardness

Figure 2 shows behavior of bubbles between two walls with the same hardness observed by a high-speed video camera. The lapsed time $t = 0$ corresponds to that at bubble formation. A bubble symmetrically divides into two parts and collapses irrespective of the wall hardness. In addition, the divided bubbles rebound, collapse several times and moves towards the wall. Figure 3 shows a time series of projected areas of bubbles. The bubble grows larger between two rigid (acrylic resin) walls than between two soft (deformable silicone rubber) walls. The collapse time for rigid walls

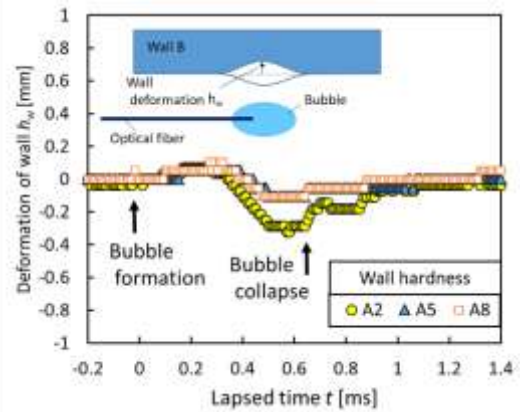
*Corresponding Author, Yasuhiro Sugimoto: y-sugi@neptune.kanazawa-it.ac.jp

becomes longer than that for soft walls. Figure 4 shows a time series of deformation on soft wall. The wall dents and bulges with bubble growth and collapse. The life time of bubbles can be affected by such slight deformation of the wall surface as shown in Fig. 3. Figure 5 shows a bubble collapse position w_c (distance from wall A) for various bubble sizes. Figure 5(a) shows the collapse position for the primary bubble and (b) for the rebound bubble, respectively. Bubble collapse positions tend to distribute around the fiber tip in the case of smaller bubble size. The bubble further moves toward the wall side with increase in maximum bubble (equivalent) radius R_{max} (where R_{max} is calculated by the projected bubble area). Furthermore, the collapse positions of the rebound bubbles are closer to the wall side than that of the primary bubbles.



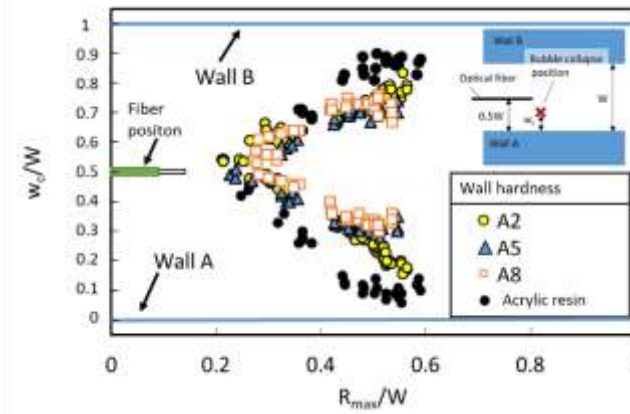
$E = 1.0 \text{ J}$, $d = 0.2 \text{ mm}$, $T_w = 297 \text{ K}$, $\beta = 7.4\text{-}7.8 \text{ mg/L}$

Fig.3 A time series of projected bubble area between walls with same hardness

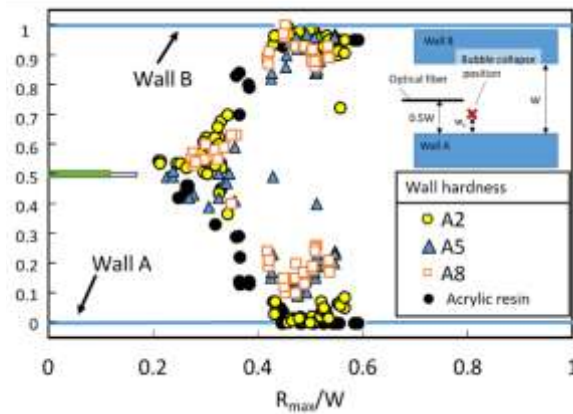


$E = 1.0 \text{ J}$, $d = 0.2 \text{ mm}$, $T_w = 296 \text{ K}$, $\beta = 7.4\text{-}7.8 \text{ mg/L}$

Fig.4 Deformation of soft wall between walls with same hardness



(a) Primary bubble collapse (1st bubble collapse)



(b) Rebound bubble collapse (2nd bubble collapse)

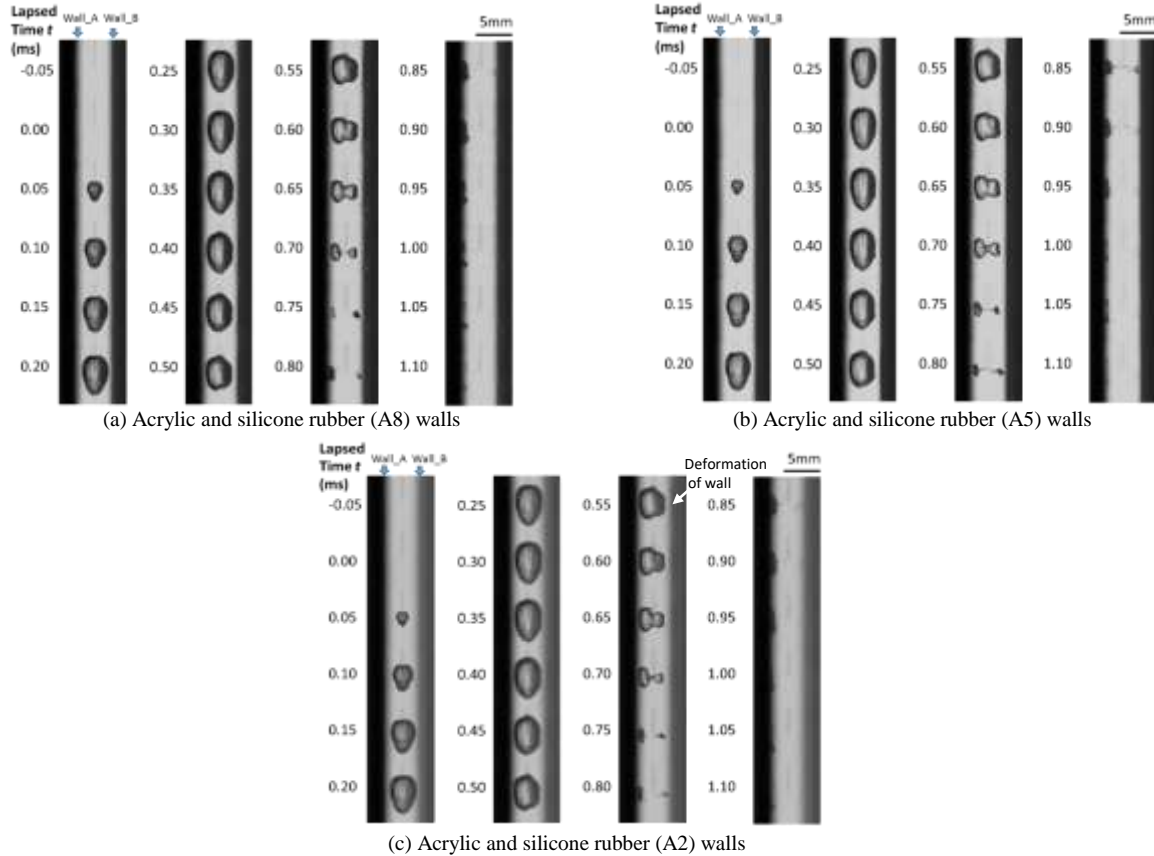
$d = 0.2 \text{ mm}$, $T_w = 297 \text{ K}$, $\beta = 7.4\text{-}7.8 \text{ mg/L}$

Fig.5 Bubble collapse positions between two walls with same hardness

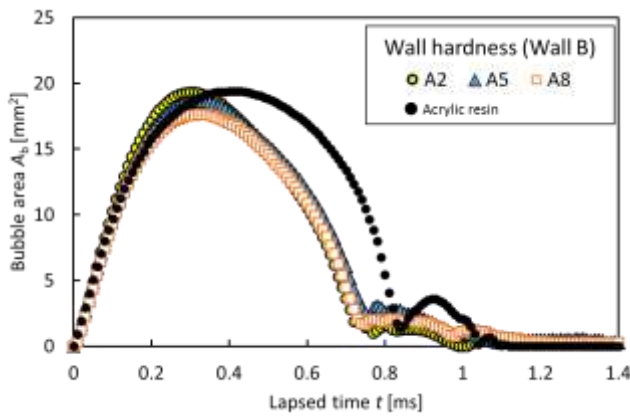
Bubble behavior between two walls with different hardness

In the case of a rigid wall and a soft wall with deformability, the bubble is asymmetrically divided even though the bubble forms at the center of two walls as shown in Fig. 6 (a) - (c). Then the larger one moves toward the rigid wall and collapses on it. This characteristic bubble collapse behavior near wall can lead to high impact [9]. The impact on the wall surface can be predicted to be larger on the rigid wall. Figure 7 shows a time series of projected bubble area. In the case of soft wall in the present study, the changes of projected bubble area show almost same tendency regardless of the wall hardness. The collapse time tends to become longer than that of walls with the same hardness as shown in Fig. 3. Figure 8 shows a time series of deformation of soft wall. The wall surface dents when the bubble grows, and it bulges so as to be sucked by the bubble deformation during bubble collapse though the deformation is small. Figure 9(a) shows the collapse position for the primary bubble and (b) for the rebound bubble in various bubble size conditions, respectively. The bubble with small radius (around $R_{max}/W = 0.2$) tends to collapse at the rigid wall side

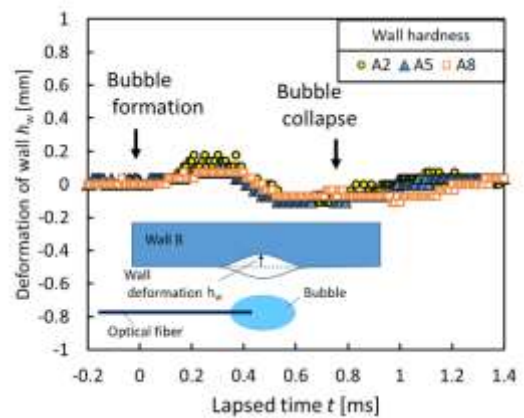
from the center. With increase in bubble size ($R_{max}/W > 0.3$) as shown in Fig. 9(a), the bubble collapse positions shift to both wall sides in any bubble size and soft wall hardness though the distribution is biased toward the hard wall side. Collapse positions of the rebound bubble are located closer to the wall side than those of the primary bubble, maintaining the asymmetric distribution as shown in Fig. 9(b). The bubble collapse pattern and position are greatly affected by wall deformation irrespective of bubble size. The bubble collapses near/on rigid wall without collapse on the soft wall around $R_{max}/W = 0.4$. This means that effective impact can act on rigid stone without damage of soft tissue.



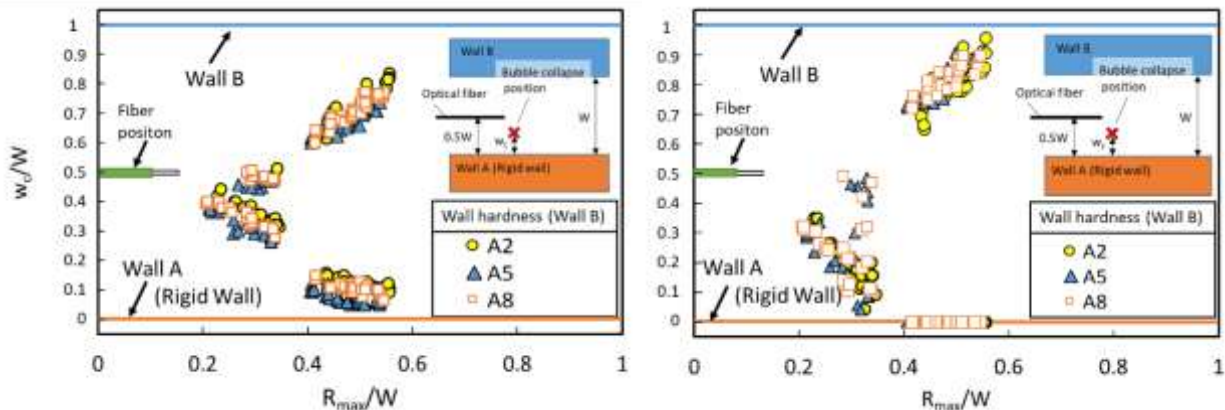
$E = 1.0 \text{ J}$, $d = 0.2 \text{ mm}$, $T_w = 296 \text{ K}$, $\beta = 7.4 \text{ mg/L}$, $f_s = 100,000 \text{ fps}$
 Fig.6 Bubble behavior between two walls with different hardness



$E = 1.0 \text{ J}$, $d = 0.2 \text{ mm}$, $T_w = 297 \text{ K}$, $\beta = 7.4-7.8 \text{ mg/L}$
 Fig.7 A time series of projected bubble area between two walls with different hardness



$E = 1.0 \text{ J}$, $d = 0.2 \text{ mm}$, $T_w = 296 \text{ K}$, $\beta = 7.4-7.8 \text{ mg/L}$
 Fig.8 Deformation of soft wall between two walls with different hardness



(a) Primary bubble collapse (1st bubble collapse) (b) Rebound bubble collapse (2nd bubble collapse)

$d = 0.2 \text{ mm}$, $T_w = 297 \text{ K}$, $\beta = 7.4\text{-}7.8 \text{ mg/L}$

Fig.9 Bubble collapse positions between two walls with different hardness

Conclusion

In order to simulate in vivo condition for TUL, we observed the bubble behavior in a narrow space between two walls with various deformability. In the case of two walls with the same hardness, a bubble symmetrically divides into two parts and collapses. The soft wall deforms due to bubble behavior such as growth and collapse. The bubble collapse position moves closer to wall during multiple bubble collapses. In the case of walls with different hardness, the bubble asymmetrically divides, moves and collapses even if the bubble begins to form at the center between two walls. The bubble collapse pattern is greatly affected even by slight wall deformation. It can be pointed out that bubble size and wall deformability play an important role in safety issues of in vivo treatment.

Acknowledgements

The authors thank to Dr. M. Moriyama, Professor of Kanazawa Medical University, and Boston Scientific Japan co., Ltd. for advice on medical view point and providing a laser equipment. A part of this work was supported by JSPS KAKENHI Grant Number JP16K06092.

References

- [1] Marks A. J., Qiu J., Milner T. E., Chan K. F. and Teichman, J. M. H. (2011). *Laser lithotripsy physics, Urinary tract stone disease*. Springer. pp.301-309.
- [2] Zhong, P. (2013). *Shock wave lithotripsy. Bubble dynamics & shock waves*. Shockwaves 8. Springer. 291-338 (ed, Delale, C. F.).
- [3] Sugimoto Y., Yamanishi Y., Sato K. and Moriyama M. (2015). *Measurement of bubble behavior and impact on solid wall induced by fiber-holmium:YAG laser*. J. Flow Control, Measurement & Visualization. 3. 135-143.
- [4] Yamanishi Y., Sugimoto Y., Sato K. (2015). *Various Conditions for Impulse Force on Solid Wall by a Fiber-type Laser Induced Bubble*. International Workshop on Cavitation Peening and Related Phenomena. 12th Int. Conf. Flow Dynamics (ICFD2015). Sendai.
- [5] Brujan, E. A., Nahen, K., Schmidt, P. and Vogel, A. (2001). *Dynamics of laser-induced cavitation bubbles near an elastic boundary*. J. Fluid Mech. 433. 251-281.
- [6] Kobayashi, K., Kodama, T., and H.Takahira. (2011). *Shock wave–bubble interaction near soft and rigid boundaries during lithotripsy: numerical analysis by the improved ghost fluid method*. Physics in Medicine & Biology. 56(19). 6421–6440.
- [7] Ogasawara, T., Tsubota, N., Seki, H., Shigaki, Y. and Takahira, H. (2015). *Experimental and numerical investigations of the bubble collapse at the center between rigid walls*. J. Physics. Conf. Ser. 656. 012031.
- [8] Mohammadzadeh, M., Mercado, J. M. and Ohl, C-D. (2015). *Bubble Dynamics in Laser Lithotripsy*. J. Physics. Conf. Ser. 656. 012004.
- [9] Tomita, Y. and Shima, A. (1986). *Mechanisms of impulsive pressure generation and damage pit formation by bubble collapse*. J. Fluid Mech. 169. 535-564.